High speed synchronous reluctance motors for electric vehicles: a focus on rotor mechanical design

Andrea Credo
Dept. of Industrial and Information Eng. and Economics
University of L'Aquila
L'Aquila, Italy
andrea.credo@graduate.univaq.it

Giuseppe Fabri
Dept. of Industrial and Information Eng. and Economics
University of L'Aquila
L'Aquila, Italy
giuseppe.fabri@univaq.it

Marco Villani
Dept. of Industrial and Information Eng. and Economics
University of L'Aquila
L'Aquila, Italy
marco.villani@univaq.it

Mircea Popescu
Motor Design Limited
Wrexham, UK
mircea.popescu@motor-design.com

Abstract— **This paper deals with the design of high-speed Synchronous Reluctance motors for electric vehicle applications. The need to enhance power density and lowering costs leads to the design of high speed motors with a reduced amount of rare earth. Pure synchronous reluctance motors potentially operate at high speed and exhibit a low cost rotor compared to PM and induction motors. Nevertheless, they present reduced performances in deep flux weakening operations in particular when the so-called radial ribs are introduced to increase the mechanical robustness of the rotor. In this paper the adoption of the radial ribs in the related design challenges are investigated and discussed. The adoption of a suitable commercial optimization tool able to optimize the placement and the sizing of the radial ribs is presented. The approach leads to an original positioning of the radial ribs able to preserve the performances of the motor at high operating speed enhancing the mechanical integrity of the rotor.**

Keywords— e-mobility, high speed, rare earth free, mechanical analysis, optimized ribs, synchronous reluctance machine, topology optimization.

I. INTRODUCTION

The electric machines have become the primary candidate for mobility [1]-[2], adopting motor solutions mainly based on high performance permanent magnets (PM) manufactured with rare-earth materials [3]-[6].

The high and volatile cost of raw materials for magnets makes uncertain their long-term availability, especially since the electric vehicle technology is going to be manufactured in mass production. Also, permanent magnet motors present several technical drawbacks that limit the performances of the motor, in particular the demagnetization effect if the temperature of the motor exceeds its operating conditions.

Therefore, there is a growing attention in alternative solutions that include rare-earth (RE) free machines or reduced RE PM machines [7]. Designers also aim to enhance the specific power of the motor-drives often by increasing their maximum operating speed.

Table 1 summarizes the main existing electric vehicles in the European & US markets, specifying the technological solution for the traction motors and their maximum operating speed.

Synchronous Reluctance Motors (SynRels) are becoming of great interest in the recent years and represent a valid alternative

TABLE I.   TRACTION MOTORS FOR ELECTRIC VEHICLE

Vehicle	Motor type	Rotor material	Max Speed [rpm]
Audi e-tron	IPMSM	RE PM	~10000
BMW i3	IPMSM	RE PM	11400
Chevrolet Bolt	IPMSM	RE PM	8900
Hyundai e-Kona	PMSM	RE PM	11000
Jaguar I-Pace	PM SynRel	Ferrite/RE PM	13000
Mercedes EQC	IPMSM	RE PM	~10000
Nissan Leaf	IPMSM	RE PM	10500
Renault Zoe	Synch. motor	Wounded Rotor	11300
Tesla S	IM	CU cage	16000

for electric and hybrid vehicles due to their simple and rugged construction. The main advantage of the SynRel relies on the absence of the rotor cage losses or PM losses, allowing a continuous torque higher than the torque of an Induction Motor (IM) of the same size [8].

Other important features are:

1) The rotor is potentially less expensive than PM motors and IM ones;

2) the specific torque is acceptable and it is not affected by the rotor temperature;

3) the field-oriented control algorithm is simpler with respect to the one of IM drives. However, accurate rotor position information is needed.

With respect to PM motors, conventional SynRels are known for their lower specific (peak) power and specific (peak) torque, higher noise and lower power factor. Despite these drawbacks, it is possible to obtain high torque density and high efficiency motors through an optimized rotor design [9]-[10]

Specific power in SynRel is enhanced by increasing the rotor operating speed and the flux-weakening region. Nevertheless, the optimal geometry for motor performances needs to be modified to guarantee the mechanical integrity of the rotor at high speed. The so-called "ribs" in tangential and radial direction are usually adopted in the classical SynRel rotor geometry (Fig. 1) to lower the mechanical stress in the rotor iron and the maximum deformation at the air-gap due to the centrifugal forces.

The paper focuses on the challenging trade-off between the electromagnetic and mechanical design aspects with reference

to the case of study aimed to design a high-speed liquid-cooled SynRel for full-electric premium vehicles.
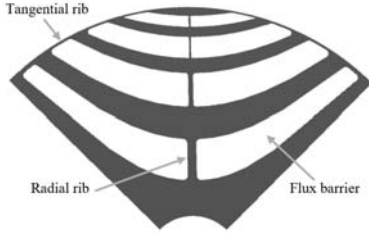

Fig. 1.   Typical view of the flux barriers and ribs in a SynRel motor.

The paper is organized as follows. Section II describes the requirements of the motor for the specific automotive application and the preliminary design, optimized from an electromagnetic point of view. Section III reports the design criteria to guarantee the rotor mechanical integrity at high speed. Section IV proposes the optimization of the positioning of the structural ribs by using a topology optimizer. The electromechanical comparison between the preliminary design and the optimized one are reported in Section V, along with the discussion of the results. Final remarks are drawn in the conclusions.

II. Optimized Electromagnetic Design of Synchronous Reluctance Motors

The design of the SynRel for traction applications requires accurate sizing procedures [11]-[12] that differ from the process of a traditional industrial machine, where it is designed to mostly operate at a nominal speed and torque. In traction motors, high performance and high efficiency are required over a wide speed range [13]; specific tools and optimization procedures [14] need to be used for the design refinement in order to satisfy the hard requirements without oversizing the machine.

The design of SynRel has to maximize the saliency ratio (L_d/L_q), achieved with several flux barriers per pole in the rotor geometry. Tangential ribs are usually included in the optimal electromagnetic design to assemble the rotor.

The saliency ratio and electromechanical torque depend also on the number of poles and, for this reason, different combinations of slots/poles need to be evaluated. According to [16] the choice of a low number of poles can reduce the q-axis inductance but it increases the torque ripple; the best solution to maximize the saliency ratio is the use of 2-poles machines (if the quality of the torque can be neglected). Whilst this is true, machines with lower number of poles have a larger stator yoke that reduces the torque density; otherwise for a high number of poles it is hard to use a high number of flux barriers and then the saliency ratio is reduced. For these reasons, the number of poles adopted in such a kind of applications is usually between 4 and 8.

Table II reports the application requirements. It is worth to highlight the high value of the torque requested at base speed (5000 rpm) and the significant value of the power request at maximum speed, where the SynRel operates in a deep flux weakening condition. It is also worth to notice the high value of

the maximum speed of the motor with respect to the available diameter and to the references in Table 1.

To reach these several requirements, "fluid shape" barriers have been chosen in order to improve the overall performance of the motor because they offer a very good saliency ratio and a reduced torque ripple. This type of rotor shape offers a favored route for the d-axis flux increasing the direct inductance, while it has the same behavior of other types of barriers (circular and rectangular) in the obstruction of the q-axis flux.

TABLE II.   MOTOR REQUIREMENTS
FOR THE TARGET APPLICATION

DC Voltage	V	800
Specific Peak Power	kW/kg	> 4.0
Specific Peak Torque	Nm/kg	> 8.0
Peak Power @5000rpm	kW	200
Peak Torque @5000rpm	Nm	380
Peak efficiency	%	> 95
Maximum speed	rpm	18000
Power @ max speed	kW	50
Motor mass	kg	< 48
Outer Stator diameter	mm	230
Stack length	mm	200
Air-gap length	mm	0.7

The analytical expression of these barriers is computed from the Joukowsky equation:

$$r(\theta) = r_{shaft} \sqrt[p]{\frac{c + \sqrt{c^2 + 4\sin^2(p\theta)}}{2\sin(p\theta)}} \qquad (1)$$

Where:

r_{shaft} is the radius of the shaft

c is a constant, function of the position of the barrier

p are the pole pairs

θ is the mechanical angle

$r(\theta)$ is the radius of the barrier curve.

To design each barrier it is necessary to define two curves and each curve is defined by a proper constant c. Because the usage of Joukowsky equation is in the matter of fact a pre-optimization of the shape of the barriers, a preliminary design was easily carried out.

The approach is effective even in the next optimization of the geometry; using the fluid shape rotor, the number of variables is limited, and the results are very promising and with an acceptable computational effort.

The pure electromagnetic optimization uses a total of 16 variables where the constraints are the peak power and the motor mass while the objective functions are the power at maximum speed and the efficiency.

In detail, nine variables have been used for the rotor: two for each barrier and one for the last one. Four variables for the stator: tooth width, yoke height, number of slots for phase for pole and

number of conductors per slot. Three general variables: stack length, current amplitude and current angle.

The cross sections of the designs optimized by the electromagnetic point of view are shown in Fig. 2, Fig. 3 and Fig. 4, respectively for the 4, 6 and 8 poles machines. The main performances are compared in Table III. Due to the constraints of the optimization all the solutions present the same peak power and motor mass, while the power at maximum speed and the efficiency are used as objective functions. The design with 6-poles presents a good starting design allowing the highest power density and the highest power at maximum speed.

Fig. 2.   Cross section of the optimal 4-poles design

Fig. 3.   Cross section of the 6-poles preliminary design

Fig. 4.   Cross section of the 8-poles preliminary design

TABLE III.   PRELIMINARY DESIGNS

Performance		4-poles	6-poles	8-poles
Peak Torque	Nm	430	430	430
Peak Power	kW	200	200	200
Peak efficiency	%	97.8	97.6	97.4
Power @ max speed (18000 rpm)	kW	94	110	78
Max phase current	A	700	700	700
Current density @ rated power	A/mm2	10.8	11.0	11.2
Maximum phase voltage	V	400	400	400
Motor mass	kg	48	47	48

III.   DESIGN CRITERIA FOR HIGH SPEED

After the electromagnetic optimization, the rotor geometry needs to be analyzed by the mechanical point of view to guarantee the integrity of the rotor over the full operating conditions; the focus is on the mechanical stress and on the deformation at the air-gap caused by the centrifugal forces.

The structure in Fig. 3, related to the optimal electromagnetic design, is obviously too weak to sustain the centrifugal force. The approach is to increase the thickness of the tangential ribs and to include radial ribs in the rotor geometry starting from the inner ones to contain the rotor deformation at the air-gap and to reduce the stress on the electrical steel.

The thickness and the number of ribs per pole increase significantly with the rotor speed to assure the mechanical integrity of the rotor. While the barrier shape is not modified compared to the optimal shape for the flux, the introduction of the ribs affects the magnetic behavior of the rotor and it globally reduces its performance. This effect happens because a large part of the magnetic flux flows through these ribs, increasing the quadrature inductance (L_q). If the thickness of the ribs is limited, the ribs are affected by a strong saturation and the effect on the motor performance is limited.

This effect is more significant in traction applications since the electric motor usually operates in heavy flux-weakening operations, in which the quadrature current is predominant with respect to the direct one. This condition leads to more restrictive voltage limits. Moreover, in premium vehicles the motor power at low speed and the one at maximum speed are fighting requirements.

Additionally, the presence of radial and tangential ribs increases the magnetic coupling between direct and quadrature axes, affecting the effectiveness of the control strategy. This leads to a reduction of the motor performances unless a non-linear model obtained by Finite Elements (FE) computation is used in the control algorithm [15].

A mechanical optimization of the thickness of the ribs has been carried out with respect to the centrifugal forces. The structural analysis was done by imposing as boundary conditions the allowable stress of the adopted electrical steel and the maximum deformation at the air-gap. The optimized rotor geometry is reported in Fig. 5 along with the computed equivalent stress. As mentioned in the discussion above, the performances of the motor are degraded by the insertion of the ribs, as reported in TABLE IV. Section IV, where the comparisons with respect to the optimal electromagnetic design are collected.
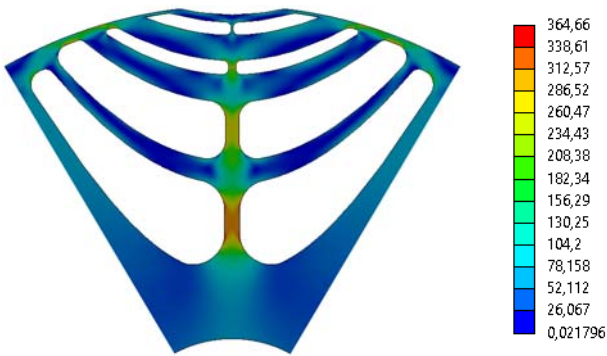
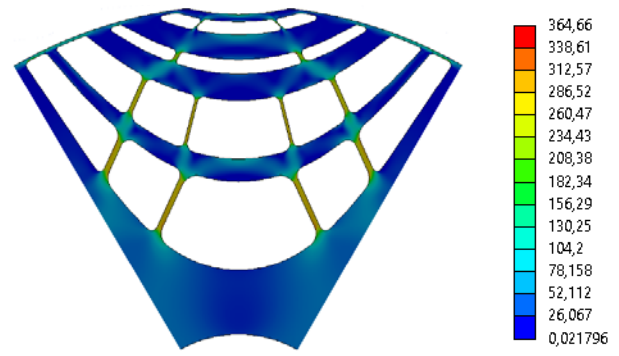Fig. 5. Radial ribs solution: mechanical stress of the 6-poles machine [MPa]

Fig. 6. SynRel motor with optimized ribs: equivalent mechanical stress [MPa]

IV. ROTOR MECHANICAL DESIGN AIDED BY A TOPOLOGY OPTIMIZATION ALGORITHM

To improve the performance of the machine and considering the maximum speed of the motor with respect to its rotor diameter it is worth to accurately analyze the effect of the centrifugal force acting on the rotor in the attempting to find a better sizing and positioning of the ribs.

Looking at the radial ribs in Fig. 4, it can be noticed that higher values of stress are visible in the ribs and the ribs thickness was increased to contain the stress within acceptable values. Hence the idea was to increase the number of the radial ribs in the attempt of reducing the ribs thickness (tangential and radial) enough to assure their saturation.

In mechanics, the reduction of the material mass falls into the class of optimization algorithms commonly referred as topology optimizers; these algorithms optimize the quantity and the positioning of the mass needed by a mechanical part to sustain the stress. The optimization of the thickness and positioning of the ribs seems to match the capabilities of these class of algorithms.

A study with a topology optimizer coupled to a mechanical FE software has been carried out on the 6-poles design in order to obtain the guidelines for the optimal positioning and the optimal thickness of the ribs to minimize the q-axis inductance. The constraints imposed are the same maximum stress and the same deformation at the air-gap of the analysis in Section III.

The optimization starts with the filling of the rotor barriers with material (rotor iron) and with the application of the mesh. Then the algorithm iteratively removes step by step the material in each mesh element in function of their stress in the attempt of minimizing the needed mass (Fig. 5).

The result of the process leads to a new rotor layout with multiple ribs in different positions with respect to the flux barriers (Fig. 4): it is clear that this geometry is quite unusual compared to those typically reported in literature.

The mechanical equivalent stress map at max speed (18000 rpm) is reported in Fig. 5, the maximum values are quite similar, so from a mechanical point of view the two design have the same performance.
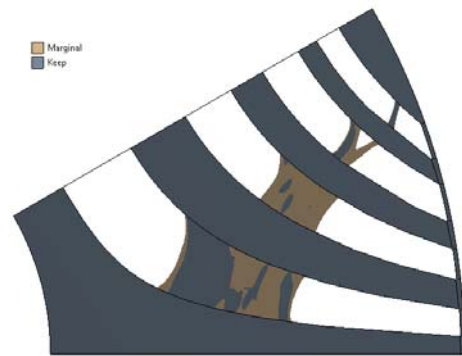

Fig. 7. Detail of the operation of the topology optimization algorithm (half pole): material removed (white), material under evaluation (brown); material to keep (grey).
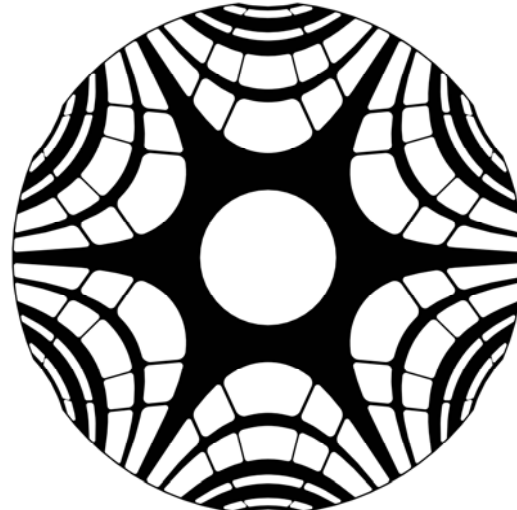

Fig. 8. New rotor shape of the 6-poles machine.

V. RESULTS AND DISCUSSION

After the topology optimization, the geometry needs a further refinement to smooth the edges and imperfections left by the optimizer, than the behavior and the performance of the machine can be analyzed.

Fig. 9 show the deformation of the rotor at the air-gap at maximum speed operation. In each cases, the deformation is less than 10% of the air-gap to avoid any risk contact between rotor and stator considering also possible fluctuation of machine due to external disturbances, tolerances and the bearings selection.

Figures 10 to 12 report the map of the flux density in the rotor respectively for the solution without radial ribs, with radial ribs and with optimized ribs at maximum speed and same phase currents. The different saturation levels of the ribs can be noticed in the three layouts. The solution with no radial ribs exhibits strong flux density levels in each of the tangential ribs, otherwise only some ribs saturate in the solution with radial ribs, in particular the thickest ones present low density. The solutions with the optimized rib allows to reduce the thickness of the tangential ribs improving the saturation, moreover the central ribs are all near the saturation and the ones in the two external barriers are well saturated.

The analysis of the saliency ratio over the speed range at the maximum performance of the machine (Fig. 13). The results confirms a better distribution of the flux when optimized ribs are used compared with the radial ribs all over the speed range while the ideal design with no ribs is still far to be equaled.

Figures 14 and 15 reports the detail of the direct and quadrature inductances related to the different designs. Both the inductances (Ld and Lq) tend to increase when the ribs are included inside the barriers increasing the voltage drops into the motor. The adoption of the optimized ribs strongly reduces the values of the inductances in the field weakening operations with respect to the radial ribs. The field weakening strategy become easier due to the reduced voltage demanded by the motor at high speed and the motor performance increases.

Fig. 16 and Fig. 17 report the performance over the speed range of the motor respectively in terms of torque and power varying the ribs adopted. The new rotor layout allows to gain up to 65% more power at high speed with respect to the classical layout based on radial ribs. Other performance are listed in Table IV, in particular the optimized layout gives also benefit for the power factor. Other considerations involve the manufacturing costs; the optimized solution are not different than preliminary one considering industrial processing because in each case it is necessary a dedicate mold for blinking and its cost does not depend from geometry.
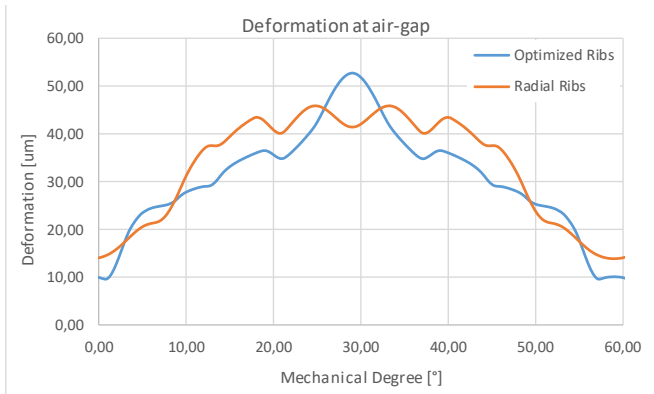

Fig. 9. Air-gap deformation of the SynRel motor: radial ribs vs optimized ribs at maximum speed.
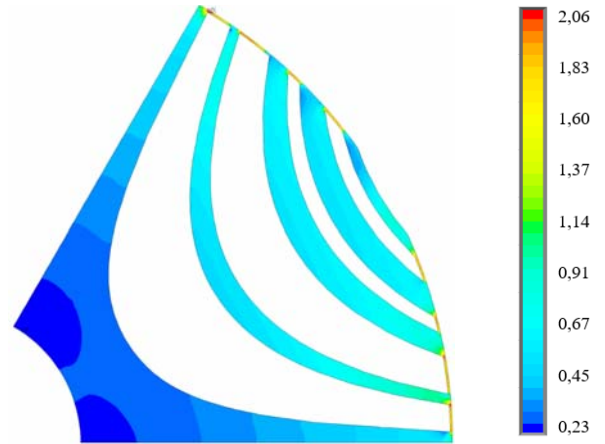

Fig. 10. SynRel motor with no radial ribs: flux density map at maximum speed [T].
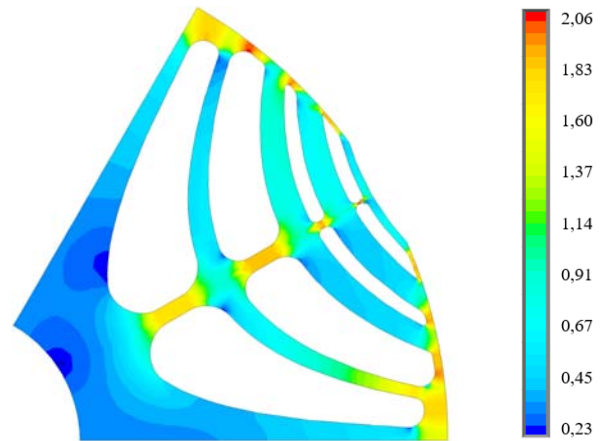

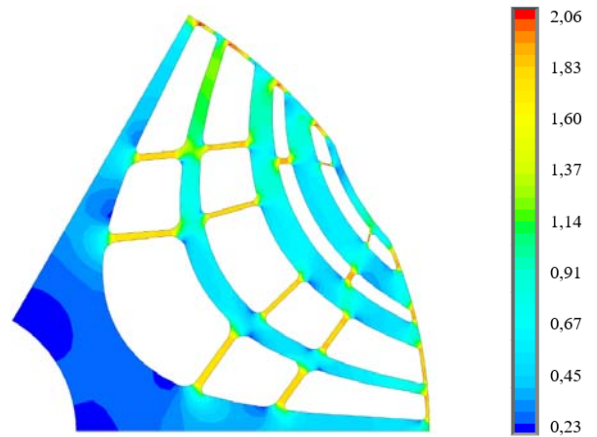Fig. 11. SynRel motor with radial ribs: flux density map at maximum speed [T].

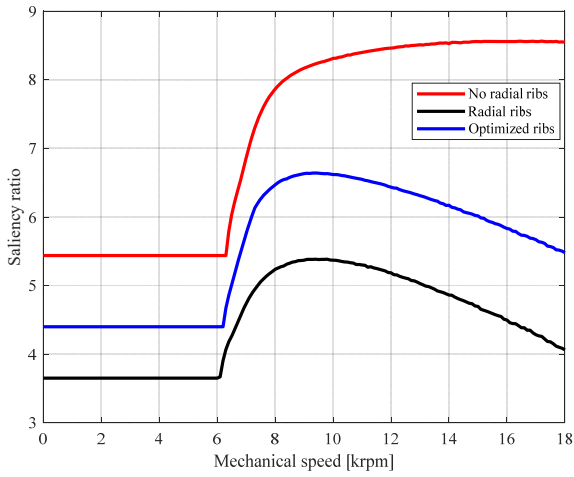Fig. 12. SynRel motor with optimized ribs flux density map at maximum speed [T].

Fig. 13. Saliency ratio over the speed range for the rotor with no radial ribs, radial ribs and optimized ribs.
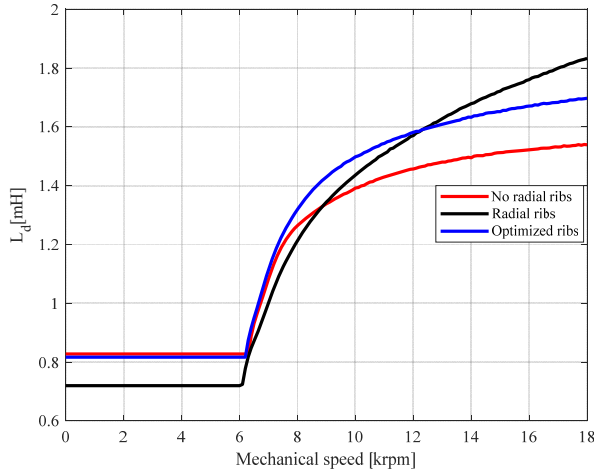

Fig. 14. Direct inductance over the speed range for the motor with no radial ribs, radial ribs and optimized ribs.
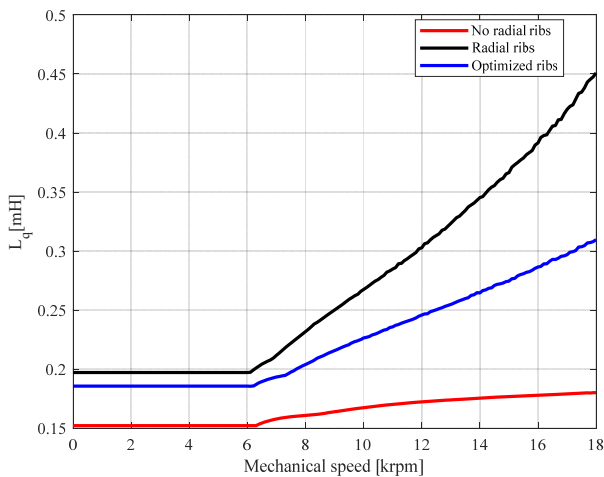

Fig. 15. Quadrature inductance over the speed range for the motor with no radial ribs, radial ribs and optimized ribs.
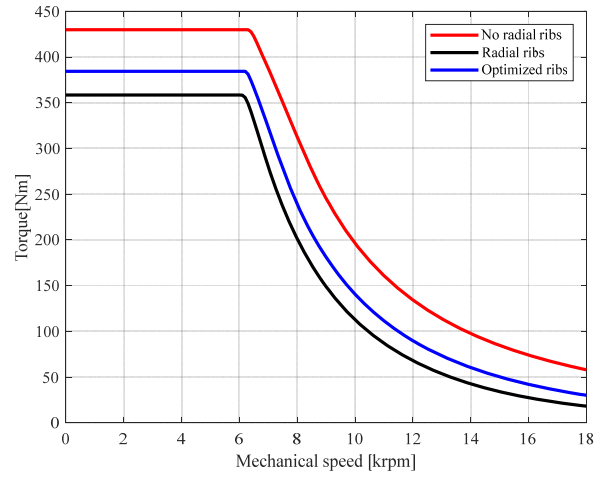

Fig. 16. Electromagnetic torque over the speed range for the motor with no radial ribs, radial ribs and optimized ribs.
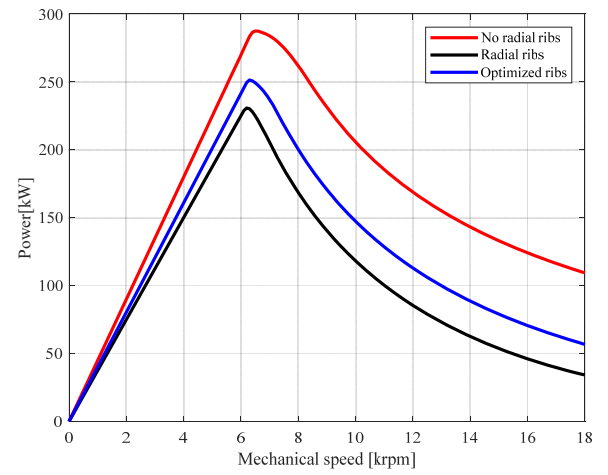

Fig. 17. Output Power over the speed range for the motor with no radial ribs, radial ribs and optimized ribs.

TABLE IV.   COMPARISON BETWEEN PRELIMINARY AND OPTIMIZED DESIGNS (6-POLES)

Performance		no radial ribs	radial ribs	optimized ribs
Peak torque	Nm	430	358	384
Peak power	kW	287	230	250
Peak efficiency	%	97.6	96.9	97.1
Power @ max speed (18000 rpm)	kW	110	35	58.5
Power factor @ 200kW		0.64	0.46	0.51
Power factor @ max speed		0.61	0.41	0.46
Max air-gap deformation	%	-	6.6	7.4
Max equivalent stress	MPa	-	364	361

CONCLUSION

Different types of motors are under evaluation for traction application in e-mobility. Synchronous Reluctance Motors are becoming of great interest in the recent years and represent a suitable alternative for their simple and rugged construction. In this study, different solutions are proposed and compared, with focus on the coupled electromagnetic and mechanical design aspects. Since the SynRel is designed with a small air-gap and its rotor geometry is mechanically weak, the containment of the rotor mechanical stress and deformation is challenging at high speed. Hence, in this study a deep mechanical analysis has been carried out with the aim to refine the rotor shape in order to achieve a better tradeoff between the rotor integrity and the motor performance. A topology optimizer has been used in order to obtain the guideline for the optimal positioning and thickness of the ribs and the impact on the performance has been detailed. The SynRel motor may not guarantee the same peak performances of IM and PM motors in automotive application especially when high speed is required. Nevertheless, an accurate design can fill the gap with other technologies and, when cost aspects are relevant it can be a valid solution. In particular, the Synchronous Reluctance motor represents a potential candidate to reduce the use of rare-earth materials in large mass production scenarios.

REFERENCES

[1] C.C.Chan, "The State of the Art of Electric and Hybrid Vehicles", Proceeding of IEEE, vol. 90, no. 2, February 2002, pp. 247-275.

[2] Z. Q. Zhu, D. Howe, "Electrical Machines and Drives for Electric, Hybrid, and Fuel Cell Vehicles", Proceedings of the IEEE, vol. 95, no. 4, April 2007, pp. 746-765.

[3] K. T. Chau, C. C. Chan, Chunhua Liu, "Overview of Permanent-Magnet Brushless Drives for Electric and Hybrid Electric Vehicles", IEEE Transaction on Industrial Electronics, vol. 55, no.. 6, June 2008, pp. 2246-2257.

[4] M.Burwell, J.Goss, M.Popescu, "Performance/cost comparison of induction motor & permanent magnet motor in a hybrid electric car", International Copper Association, July 2013, Tokyo.

[5] J.R. Hendershot and T.J. E. Miller, Design of Brushless Permanent-Magnet machines, Motor Design Books LLC, 2010.

[6] E. Arfa Grunditz, T. Thiringer, "Performance Analysis of Current BEVs Based on a Comprehensive Review of Specifications", IEEE Trans. On Transportation Electrification, Vol. 2, No. 3, September 2016.

[7] J. D.Widmer , R. Martin, M. Kimiabeigi, "Electric vehicle traction motors without rare earth magnets", Sustainable Materials and Technologies, Elsevier, 3 (2015), pp. 7-13.

[8] M. Villani, M. Tursini, M. Popescu, G. Fabri, A. Credo, L. Di Leonardo "Experimental Comparison between Induction and Synchronous Reluctance Motor-Drives" ICEM 2018, XXIII International Conference on Electrical Machines, Alexandroupoli (Greece), September 2018,

[9] M. Ferrari, N. Bianchi, A. Doria and E. Fornasiero, "Design of Synchronous Reluctance Motor for Hybrid Electric Vehicles", IEEE Transactions on Industry Applications, vol. 51, no. 4, pp. 3030-3040, 2015.

[10] M. Tursini, M. Villani, G. Fabri, A. Credo, F. Parasiliti and A. Abdelli, "Synchronous Reluctance Motor: Design, Optimization and Validation", SPEEDAM, International Symposium on Power Electronics, Electrical Drives, Automation and Motion, Amalfi (Italy), June 2018.

[11] G. Pellegrino, F. Cupertino and C. Gerada, "Automatic Design of Synchronous Reluctance Motors Focusing on Barrier Shape Optimization", IEEE Transactions on Industry Applications, vol. 51, no. 2, pp. 1465-1474, 2015.

[12] F.Parasiliti, M.Villani "Magnetic analysis of flux barriers Synchronous Reluctance Motors" ICEM 2008, XVIII International Conference on Electrical Machines, Vilamoura (Portugal), September 2008.

[13] I. Boldea, L. Tutelea, L. Parsa and D. Dorrell, "Automotive Electric Propulsion Systems With Reduced or No Permanent Magnets: An Overview", IEEE Transactions on Industrial Electronics, vol. 61, no. 10, pp. 5696-5711, 2014.

[14] S.Lucidi, F.Parasiliti, F.Rinaldi, M.Villani "Finite Element Based Multi-Objective Design Optimization Procedure of Interior Permanent Magnet Synchronous Motors for Wide Constant-Power Region Operation", IEEE Trans. on Industrial Electronics, vol. 59, p. 2503-2514, ISSN: 0278-0046.

[15] M. Tursini, M. Villani, G. Fabri, S. Paolini, A. Credo and A. Fioravanti, "Sensorless control of a synchronous reluctance motor by finite elements model results", SLED IEEE International Symposium on Sensorless Control for Electrical Drive, Catania (Italy), September 2017.

[16] S. Taghavi, P. Pillay, "A Sizing Methodology of the Synchronous Reluctance Motor for Traction Applications", IEEE Journal of Emerging and Selected Topics in Power Electronics, Vol.. 2, No. 2, June 2014

.